

# Computer Modelling and Circuit Design of a new 8D Chaotic System

Michael Kopp <sup>1</sup> and Andrii Kopp <sup>2</sup>

<sup>1</sup>Institute for Single Crystals

<sup>2</sup>Affiliation not available

October 30, 2023

## Abstract

In this paper, Matlab-Simulink and LabView models are constructed for a new nonlinear dynamic system of equations in an eight-dimensional (8D) phase space. For fixed parameters of the 8D dynamical system, the spectrum of Lyapunov exponents and the Kaplan-York dimension are calculated. The presence of two positive Lyapunov exponents demonstrates the hyperchaotic behavior of the 8D dynamical system. The fractional Kaplan-York dimension indicates the fractal structure of strange attractors. We have shown that an adaptive controller is used to stabilize the novel 8D chaotic system with unknown system parameters. An active control method is derived to achieve global chaotic synchronization of two identical novel 8D chaotic systems with unknown system parameters. Based on the results obtained in Matlab-Simulink and LabView models, a chaotic signal generator for the 8D chaotic system is implemented in the Multisim environment. The results of chaotic behavior simulation in the Multisim environment show similar behavior when comparing simulation results in Matlab-Simulink and LabView models.

# Computer Modelling and Circuit Design of a new 8D Chaotic System

Michael Kopp<sup>1</sup>, Andrii Kopp<sup>2</sup>

<sup>1</sup>*Institute for Single Crystals, NAS Ukraine, Kharkiv, Ukraine*

<sup>2</sup>*National Technical University "Kharkiv Polytechnic Institute", Kharkiv, Ukraine*

(\*Corresponding author's e-mail: [michaelkopp0165@gmail.com](mailto:michaelkopp0165@gmail.com))

## Abstract

In this paper, Matlab-Simulink and LabView models are constructed for a new nonlinear dynamic system of equations in an eight-dimensional (8D) phase space. For fixed parameters of the 8D dynamical system, the spectrum of Lyapunov exponents and the Kaplan-York dimension are calculated. The presence of two positive Lyapunov exponents demonstrates the hyperchaotic behavior of the 8D dynamical system. The fractional Kaplan-York dimension indicates the fractal structure of strange attractors. We have shown that an adaptive controller is used to stabilize the novel 8D chaotic system with unknown system parameters. An active control method is derived to achieve global chaotic synchronization of two identical novel 8D chaotic systems with unknown system parameters. Based on the results obtained in Matlab-Simulink and LabView models, a chaotic signal generator for the 8D chaotic system is implemented in the Multisim environment. The results of chaotic behavior simulation in the Multisim environment show similar behavior when comparing simulation results in Matlab-Simulink and LabView models.

**Keywords:** chaotic behavior, chaos generator, computer simulation, circuit simulation.

## Introduction

It is well known that deterministic chaos is widely used in several engineering problems with the design of telecommunication systems [1,2]. The implementation of electronic circuits for new chaos generators makes it possible to carry out physical modeling of the equations of nonlinear dynamics as an alternative to numerical modeling. One of the most popular examples of a dynamical system with chaotic behavior is the Lorentz system [3] describing the phenomenon of free convection in an atmosphere. In the work [4], an electronic circuit of Lorentz equations was implemented. This circuit generates chaotic signals, which behavior closely corresponds to the results predicted by numerical experiments. The paper [4] demonstrates an approach to secure data exchange using the concept of synchronized chaotic systems. The Lorenz scheme is implemented both in the transmitter and receiver. A chaotic masking signal is added at the transmitter to the informational message (modulation process), and the informational message is recovered (demodulation process) by subtracting the chaotic signal generated in the receiver.

There has been increasing interest in exploiting chaotic dynamics in engineering applications. Due to the work [4] the creation of electronic chaos generators was stimulated. Electronic generators of chaos immediately appeared based on Rössler equations [5,6], Rikitake equations [7], modified Lorentz equations [8-11], Rucklidge equations [12]. Recently, new systems with hyperchaotic oscillations have been developed such as Liu systems [13-14], Chen systems [15] and new modifications of the Lorentz equations [16-17] and Rikitake equations [18-20]. The book [21] is devoted to an overview of chaos generators based on circuit simulation using the Multisim package. Such systems are characterized by broadband, orthogonality, and complexity of the structure of chaotic signals, as well as strong sensitivity to initial conditions. These properties determine perspectives for their use for the secure transmission of information.

In this paper, we consider the equations of nonlinear 8D dynamics that describe convection in a nonuniformly rotating electrically conductive fluid in a helical magnetic field [22]. These equations were obtained similarly to the Lorentz equations [3] using the representation of physical fields in the form of expansions of the Fourier series of the minimum order. However, in contrast to the Lorentz equations

(3D), we have obtained a nonlinear dynamic system of equations of a higher dimension of the phase space (8D) [22]. Chaotic systems with an attractor of dimensions above 3D have a much wider practical application. It is preferred to use chaotic systems of a higher dimension for secure communication. The chaotic system has more complex dynamics in the presence of more than one Lyapunov exponent, which increases the security of information transmission. In addition, such systems are characterized by broadband, orthogonality, and complexity of the structure of chaotic signals, as well as strong sensitivity to initial conditions. These properties determine perspectives for their use for the secure transmission of information. Therefore, computer simulation of chaotic signals and the search for a circuit implementation of chaotic oscillation generators is an important problem.

The purpose of this paper is to construct computer models of a chaotic dynamic system (8D) using the Matlab-Simulink environment and the LabView software environment. For the circuit implementation of the new chaos generator, we use the NI Multisim package, where chaotic dynamics are illustrated by signal oscillograms and phase portraits of attractors.

## Materials and methods

### Basic equations of the 8D chaotic system

The dynamic system of equations describing weakly non-linear convection in a nonuniformly rotating electrically conductive fluid in a helical magnetic field has the following form [22]

$$\begin{cases} \dot{X} = -X + RY - TV - HU + \tilde{H}\tilde{W} \\ \dot{V} = -V + HW + \sqrt{Ta}(1 + Ro)X \\ \dot{\tilde{V}} = -\tilde{V} + \tilde{\xi}H(1 + Rb)U - H\tilde{W} \\ \dot{U} = -Pm^{-1}U + Pr^{-1}X \\ \dot{W} = -Pm^{-1}W - Pr^{-1}V + Ro\sqrt{Ta}U \\ \dot{\tilde{W}} = -Pm^{-1}\tilde{W} + Pr^{-1}\tilde{V} + \tilde{\xi}Pr^{-1}RbX \\ \dot{Y} = Pr^{-1}(-Y + X - XZ) \\ \dot{Z} = Pr^{-1}(-bZ + XY) \end{cases} \quad (1)$$

where the dot on the symbol indicates the differentiation with respect to time  $t$ .  $X, V, \tilde{V}$  are amplitudes of disturbances of velocity fields,  $U, W, \tilde{W}$  are amplitudes of disturbances of magnetic fields,  $Y, Z$  are amplitudes of disturbances of temperature fields. Parameters  $H, \tilde{H}, Ta, T, Pm, Pr, Ro, \tilde{\xi}, b$  are real constants, and  $R$  (the Rayleigh number) is a bifurcation parameter. The last two nonlinear equations in system (1) are similar to similar equations in the Lorentz system [3]. Therefore, the nonlinear system of equations (1) similar to equations of Lorentz type for eight-dimensional 8D phase space. In the limiting case, when there is only a constant external axial magnetic field, equations (1) go over to the Lorentz equations for the six-dimensional 6D phase space, which were numerically investigated in [23]. The nonlinear equations system (1) describes trajectory movement in 8D-dimensional phase space and depends on the large number of dimensionless parameters (11 parameters):  $H, \tilde{H}, Ta, T, Pm, Pr, Ro, \tilde{\xi}, b$ .

Equations (1) have a huge variety of multiple behavior modes. More likely, that it can realize all possible transitions to chaos depending on the area of changes of various dimensionless parameters:  $H, \tilde{H}, Ta, T, Pm, Pr, Ro, \tilde{\xi}, b$ . In the work [22], a dynamic analysis of the system (1) was performed. The existence of periodic, quasi-periodic and chaotic regimes was proved depending on the values of the Rayleigh number. Considering the large number of parameters it can be assumed, that in the system of equations (1) are implemented most of the nowadays known scenarios of transition to the chaos, if not all of them. The scenario of doubling of the Feigenbaum period is changed with the subharmonic Sharkovsky cascade, and then with the homoclinic cascade of bifurcations [22].

Using the values of the parameters

$$H = 2, Ta = 1080, T = 0.1, Pm = 1, Pr = 10, b = 8/3, \tilde{H} = 0.06, \tilde{\xi} = 9.4, Rb = 1/2, Ro = -3/4 \quad (2)$$

we write the system (1) in a form more convenient for modeling:

$$\begin{cases} \dot{x}_1 = -x_1 + Rx_2 - 2x_4 - 0.1x_5 \\ \dot{x}_2 = \frac{1}{10}(-x_2 + x_1 - x_1x_3) \\ \dot{x}_3 = \frac{1}{10}\left(-\frac{8}{3}x_3 + x_1x_2\right) \\ \dot{x}_4 = -x_4 + \frac{1}{10}x_1 \\ \dot{x}_5 = -x_5 + 8.21x_1 + 2x_6 \\ \dot{x}_6 = -x_6 - 24.65x_4 - \frac{1}{10}x_5 \\ \dot{x}_7 = -x_7 + 28.2x_4 - 2x_8 \\ \dot{x}_8 = -x_8 + 0.47x_1 + \frac{1}{10}x_7 \end{cases} \quad (3)$$

Here new variables were introduced:  $x_1 = X, x_2 = Y, x_3 = Z, x_4 = U, x_5 = V, x_6 = W, x_7 = \tilde{V}, x_8 = \tilde{W}$ . Equations (3) are supplemented with initial conditions [21]:  $x_1(0) = x_2(0) = x_3(0) = x_4(0) = x_5(0) = x_6(0) = x_7(0) = x_8(0) = 1$ . Equations (3) contain one parameter  $R$ , whose change allows us to consider a one-parameter set of solutions. The Rayleigh number  $R$  depends on the temperature difference at the boundaries of the electrically conductive fluid layer. By changing the heating conditions at the boundaries of the fluid layer (the Rayleigh number), it is possible to study various modes of convective instability. Further, we will be interested in the chaotic behavior of system (3) for the value of parameter  $R = 58$ .

#### *Lyapunov exponents and Kaplan-Yorke dimension*

One of the important criteria characterizing the chaotic behavior of a nonlinear dynamical system is the spectrum of Lyapunov exponents. With the help of the Lyapunov exponents, the rate of convergence or divergence of trajectories in the phase space is determined. The presence of at least one positive value in the spectrum of Lyapunov exponents indicates the presence of chaotic oscillations in the system. The number of Lyapunov exponents corresponds to the dimension of the phase space of the nonlinear dynamical system. For our system (3) the number of such indicators is six. We use the method of calculating Lyapunov exponents based on the Benettin algorithm [24,25]. Following the works [26,27], we calculated the maximum Lyapunov exponent for the system of equations (3) at  $R = 58$ :  $L_{max} = 0.0974135$ , and then using the Gram-Schmidt orthogonalization more correctly determined all Lyapunov exponents

$$\begin{aligned} L_1 = 0.0914666, L_2 = 0.0232093, L_3 = -0.549477, L_4 = -0.983332, \\ L_5 = -1.01154, L_6 = -1.01105, L_7 = -1.15546, L_8 = -1.77049 \end{aligned} \quad (4)$$

We see that the spectrum of Lyapunov exponents (4) has two positive terms  $L_1, L_2$ , so the system (3) shows hyperchaotic behavior. The maximum Lyapunov exponent of the new hyperchaotic system (3) corresponds to the value  $L_{max} = 0.0914666$ . The sum of the Lyapunov exponents in (4) is negative  $L_1 + L_2 + L_3 + L_4 + L_5 + L_6 = -6.36667 < 0$ , which shows that the hyperchaotic system (3) is dissipative. The Kaplan-York dimension of the new hyperchaotic system (3) is calculated as

$$D_{KY} = 2 + \frac{L_1 + L_2}{|L_3|} \approx 2.20184 \quad (5)$$

This shows the high complexity of the system (3). **Figure 1** depicts the dynamics of the Lyapunov exponents of the hyperchaotic system (3).

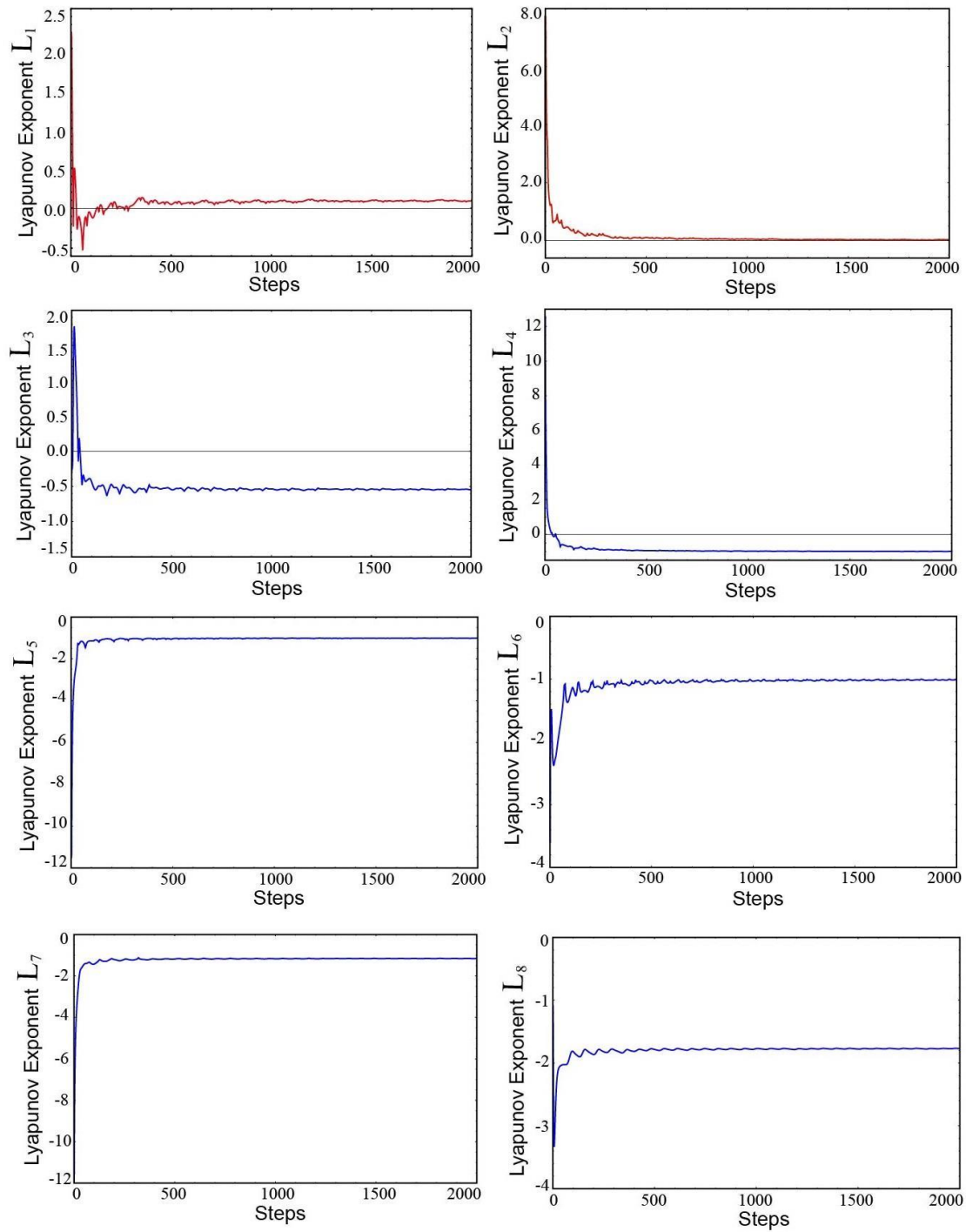


**Figure 1** Convergence plot of the Lyapunov spectrum for the system (3).

#### *Adaptive control of the 8D chaotic system*

In this section, we are considered an adaptive controller to stabilize the chaotic system (3) with unknown system parameter  $R$ . Let us represent system (3) in the following form

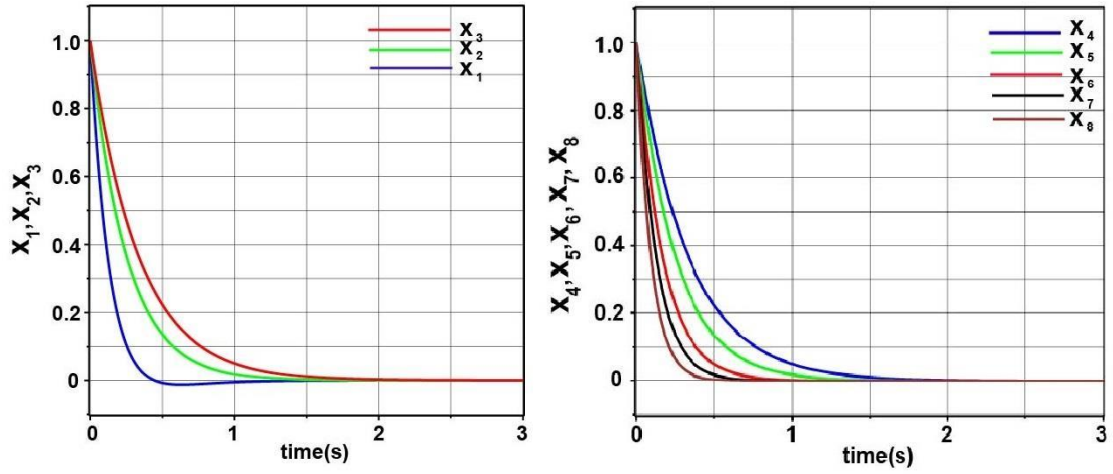


**Figure 2** Time history of the controlled chaotic system.

$$\begin{cases}
 \dot{x}_1 = -x_1 + Rx_2 - 2x_4 - 0.1x_5 + u_1 \\
 \dot{x}_2 = \frac{1}{10}(-x_2 + x_1 - x_1x_3) + u_2 \\
 \dot{x}_3 = \frac{1}{10}\left(-\frac{8}{3}x_3 + x_1x_2\right) + u_3 \\
 \dot{x}_4 = -x_4 + \frac{1}{10}x_1 + u_4 \\
 \dot{x}_5 = -x_5 + 8.21x_1 + 2x_6 + u_5 \\
 \dot{x}_6 = -x_6 - 24.65x_4 - \frac{1}{10}x_5 + u_6 \\
 \dot{x}_7 = -x_7 + 28.2x_4 - 2x_8 + u_7 \\
 \dot{x}_8 = -x_8 + 0.47x_1 + \frac{1}{10}x_7 + u_8
 \end{cases} \quad (6)$$

where  $u_1, u_2, u_3, u_4, u_5, u_6, u_7, u_8$  are adaptive controls to be determined using estimate  $R(t)$  for the unknown parameter  $R$ . We consider the adaptive feedback control law

$$\begin{cases}
 u_1 = x_1 - R(t)x_2 + 2x_4 + 0.1x_5 - k_1x_1 \\
 u_2 = \frac{1}{10}(x_2 - x_1 + x_1x_3) - k_2x_2 \\
 u_3 = \frac{1}{10}\left(\frac{8}{3}x_3 - x_1x_2\right) - k_3x_3 \\
 u_4 = x_4 - \frac{1}{10}x_1 - k_4x_4 \\
 u_5 = x_5 - 8.21x_1 - 2x_6 - k_5x_5 \\
 u_6 = x_6 + 24.65x_4 + \frac{1}{10}x_5 - k_6x_6 \\
 u_7 = x_7 - 28.2x_4 + 2x_8 - k_7x_7 \\
 u_8 = x_8 - 0.47x_1 - \frac{1}{10}x_7 - k_8x_8
 \end{cases} \quad (7)$$

In (7),  $k_1, k_2, k_3, k_4, k_5, k_6, k_7, k_8$  are positive constants.  $R(t)$  is estimate for the unknown system parameter  $R$ . Substituting (7) into (6), we get

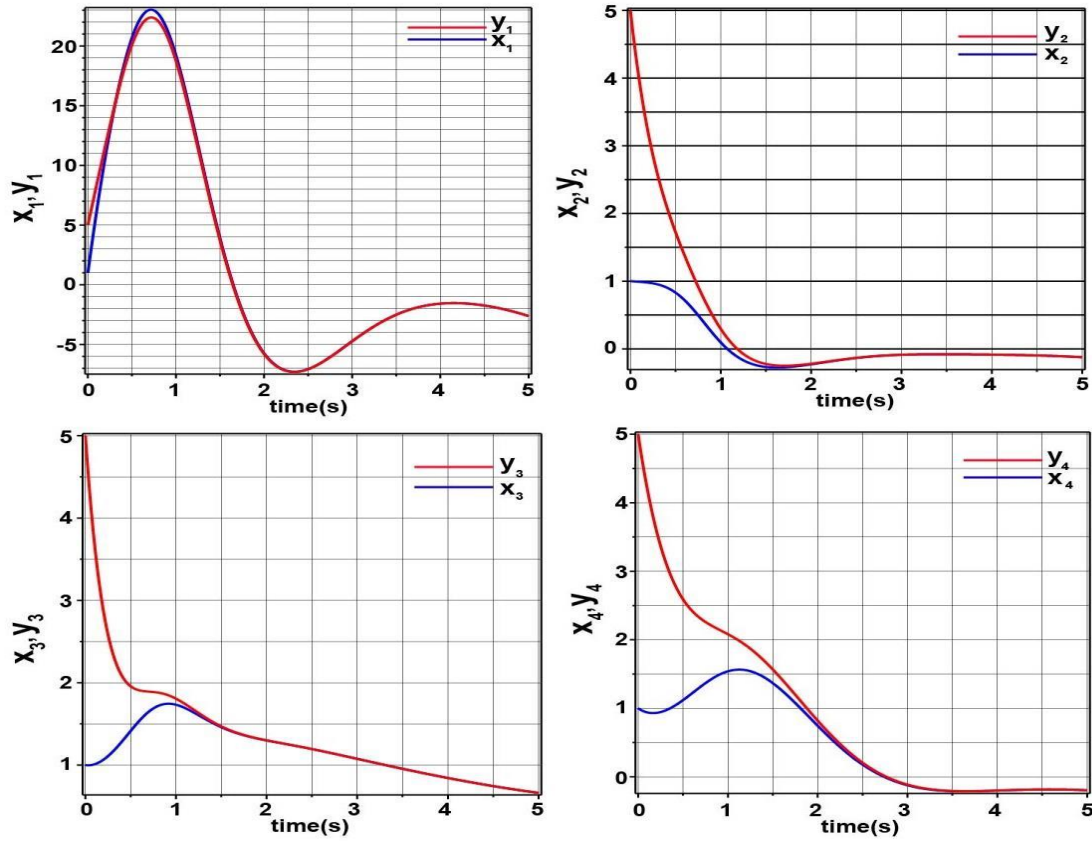


**Figure 3** Synchronization of the states  $x_1 - y_1, x_2 - y_2, x_3 - y_3, x_4 - y_4$  of the chaotic systems.

$$\begin{cases} \dot{x}_1 = (R - R(t))x_2 - k_1 x_1 \\ \dot{x}_2 = -k_2 x_2 \\ \dot{x}_3 = -k_3 x_3 \\ \dot{x}_4 = -k_4 x_4 \\ \dot{x}_5 = -k_5 x_5 \\ \dot{x}_6 = -k_6 x_6 \\ \dot{x}_7 = -k_7 x_7 \\ \dot{x}_8 = -k_8 x_8 \end{cases} \quad (8)$$

Then the parameter estimation error is defined by  $e = R - R(t)$ . After differentiating  $e$  with respect to  $t$ , we get

$$\frac{de}{dt} = -\frac{dR(t)}{dt} \quad (9)$$

Let's use adaptive control theory, we introduce Lyapunov function defined by

$$\Lambda = \frac{1}{2} (x_1^2 + x_2^2 + x_3^2 + x_4^2 + x_5^2 + x_6^2 + x_7^2 + x_8^2 + e^2) \quad (10)$$

It's obvious,  $V$  is a positive definite function. Differentiating  $V$  from (10), we can obtain

$$\frac{d\Lambda}{dt} = e \left( x_1 x_2 - \frac{dR(t)}{dt} \right) - k_i^2 x_i^2, (i = 1, 2, 3, 4, 5, 6, 7, 8) \quad (11)$$

From (11), we obtain the parameter update law as:

$$\frac{dR(t)}{dt} = x_1 x_2 \quad (12)$$

Thus, the 8D chaotic system (3) with unknown system parameter  $R$  is globally and exponentially stabilized for all initial conditions by the adaptive control law (7) and the parameter update law (12).

#### Adaptive Synchronization of the Identical 8D Chaotic System

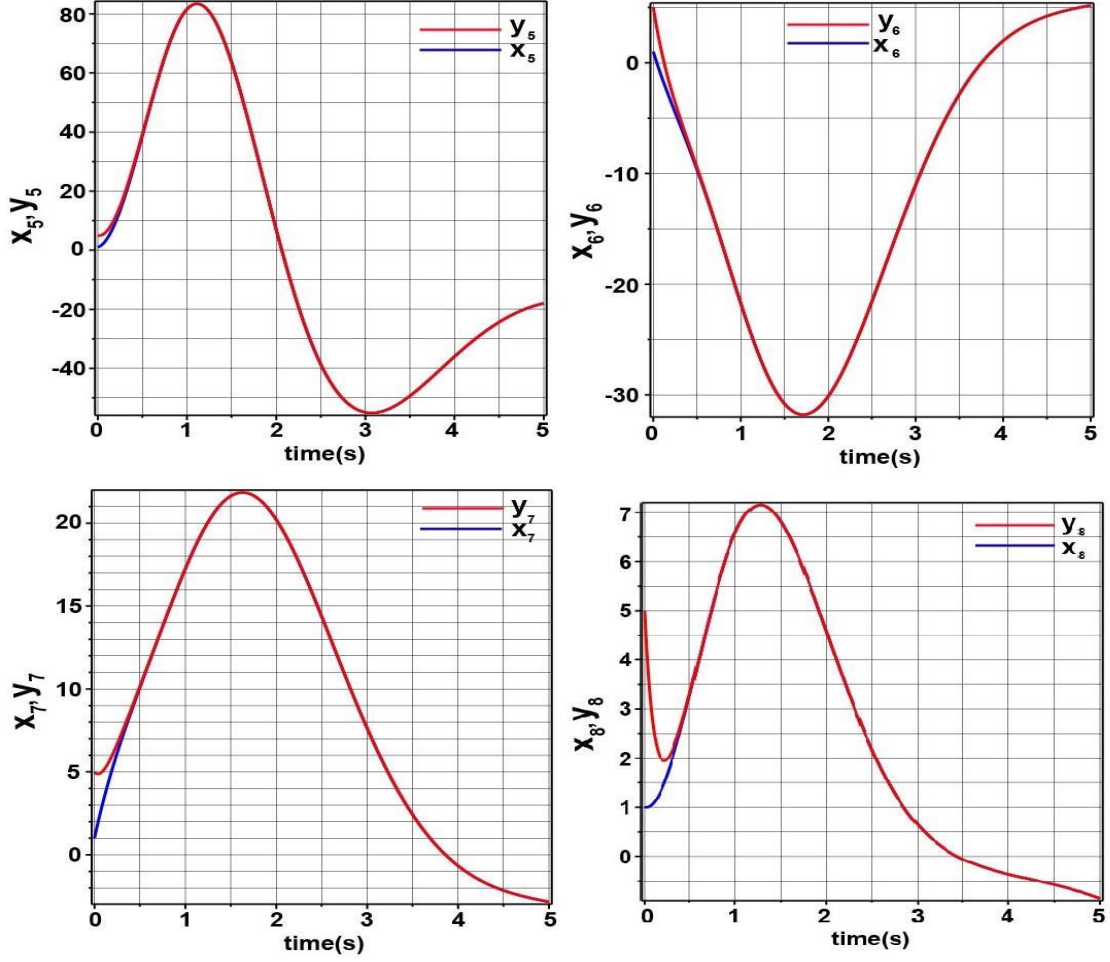


**Figure 4** Synchronization of the states  $x_5 - y_5, x_6 - y_6, x_7 - y_7, x_8 - y_8$  of the chaotic systems.

Let us consider the adaptive synchronization of identical 8D chaotic systems with unknown system parameter  $R$ . As the drive system, we take the system (3) and as the response system we take the following system

$$\begin{cases} \dot{y}_1 = -y_1 + Ry_2 - 2y_4 - 0.1y_5 + u_1 \\ \dot{y}_2 = \frac{1}{10}(-y_2 + y_1 - y_1y_3) + u_2 \\ \dot{y}_3 = \frac{1}{10}\left(-\frac{8}{3}y_3 + y_1y_2\right) + u_3 \\ \dot{y}_4 = -y_4 + \frac{1}{10}y_1 + u_4 \\ \dot{y}_5 = -y_5 + 8.21y_1 + 2y_6 + u_5 \\ \dot{y}_6 = -y_6 - 24.65y_4 - \frac{1}{10}y_5 + u_6 \\ \dot{y}_7 = -y_7 + 28.2y_4 - 2y_8 + u_7 \\ \dot{y}_8 = -y_8 + 0.47y_1 + \frac{1}{10}y_7 + u_8 \end{cases} \quad (13)$$

where  $y_1, y_2, y_3, y_4, y_5, y_6, y_7, y_8$  are the states and  $u_1, u_2, u_3, u_4, u_5, u_6, u_7, u_8$  are the controllers to be designed so as to achieve global chaos synchronization between systems (3) and (13). The synchronization error between the identical chaotic systems is defined as  $\xi_i = y_i(t) - x_i(t)$ , ( $i = 1, 2, 3, 4, 5, 6, 7, 8$ ).

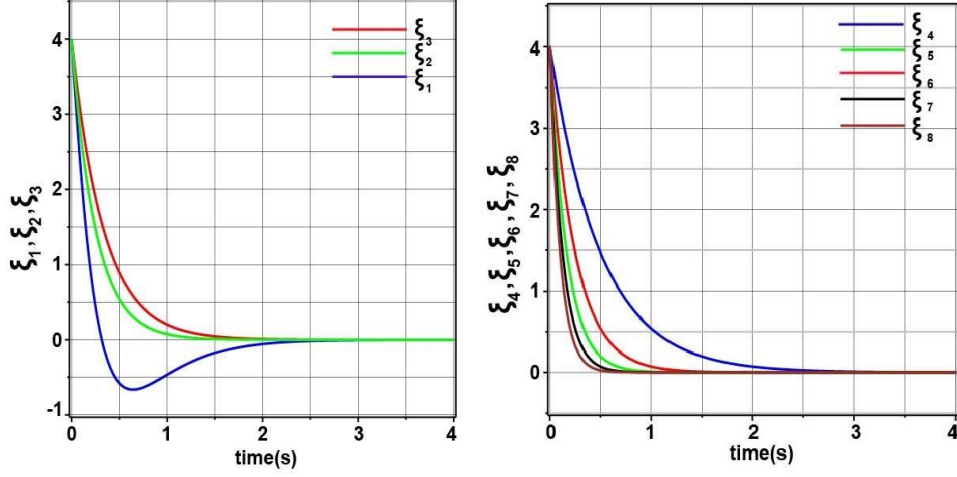


**Figure 5** Time-history of the synchronization errors.

$$\begin{cases}
 \dot{\xi}_1 = -\xi_1 + R\xi_2 - 2\xi_4 - 0.1\xi_5 + u_1 \\
 \dot{\xi}_2 = \frac{1}{10}(-\xi_2 + \xi_1 - (y_1 y_3 - x_1 x_3)) + u_2 \\
 \dot{\xi}_3 = \frac{1}{10}\left(-\frac{8}{3}\xi_3 + (y_1 y_2 - x_1 x_2)\right) + u_3 \\
 \dot{\xi}_4 = -\xi_4 + \frac{1}{10}\xi_1 + u_4 \\
 \dot{\xi}_5 = -\xi_5 + 8.21\xi_1 + 2\xi_6 + u_5 \\
 \dot{\xi}_6 = -\xi_6 - 24.65\xi_4 - \frac{1}{10}\xi_5 + u_6 \\
 \dot{\xi}_7 = -\xi_7 + 28.2\xi_4 - 2\xi_8 + u_7 \\
 \dot{\xi}_8 = -\xi_8 + 0.47\xi_1 + \frac{1}{10}\xi_7 + u_8
 \end{cases} \quad (14)$$

We write the adaptive control law

$$\begin{cases}
 u_1 = \xi_1 - R(t)\xi_2 + 2\xi_4 + 0.1\xi_5 - k_1\xi_1 \\
 u_2 = \frac{1}{10}(\xi_2 - \xi_1 + (y_1 y_3 - x_1 x_3)) - k_2\xi_2 \\
 u_3 = \frac{1}{10}\left(\frac{8}{3}\xi_3 - (y_1 y_2 - x_1 x_2)\right) - k_3\xi_3 \\
 u_4 = \xi_4 - \frac{1}{10}\xi_1 - k_4\xi_4 \\
 u_5 = \xi_5 - 8.21\xi_1 - 2\xi_6 - k_5\xi_5 \\
 u_6 = \xi_6 + 24.65\xi_4 + \frac{1}{10}\xi_5 - k_6\xi_6 \\
 u_7 = \xi_7 - 28.2\xi_4 + 2\xi_8 - k_7\xi_7 \\
 u_8 = \xi_8 - 0.47\xi_1 - \frac{1}{10}\xi_7 - k_8\xi_8
 \end{cases} \quad (15)$$

where  $k_1, k_2, k_3, k_4, k_5, k_6, k_7, k_8$  are positive constants controlling the synchronization speed,  $R(t)$  is estimate of the unknown parameter  $R$ . The parameter estimation error is defined by  $e_R = R - R(t)$ . As a result, we get the error dynamics

$$\begin{cases} \dot{\xi}_1 = (R - R(t))\xi_2 - k_1\xi_1 \\ \dot{\xi}_2 = -k_2\xi_2 \\ \dot{\xi}_3 = -k_3\xi_3 \\ \dot{\xi}_4 = -k_4\xi_4 \\ \dot{\xi}_5 = -k_5\xi_5 \\ \dot{\xi}_6 = -k_6\xi_6 \\ \dot{\xi}_7 = -k_7\xi_7 \\ \dot{\xi}_8 = -k_8\xi_8 \end{cases} \quad (16)$$

Next, we consider the quadratic Lyapunov function defined by

$$\Lambda = \frac{1}{2}(\xi_1^2 + \xi_2^2 + \xi_3^2 + \xi_4^2 + \xi_5^2 + \xi_6^2 + \xi_7^2 + \xi_8^2 + e_R^2) \quad (17)$$

Taking into account that  $\dot{e}_R = -dR(t)/dt$ , we find

$$\frac{d\Lambda}{dt} = \left( \xi_1\xi_2 - \frac{dR(t)}{dt} \right) e_R - k_i\xi_i^2, \quad (i = 1, 2, 3, 4, 5, 6, 7, 8) \quad (18)$$

From (18) we obtain the parameter update law as:

$$\frac{dR(t)}{dt} = \xi_1\xi_2 \quad (19)$$

Therefore, the identical novel chaotic systems (3) and (13) with unknown system parameter is globally and exponentially synchronized for all initial conditions by the adaptive control law (15) and the parameter update law (19). In other words according to Lyapunov's stability theory, if  $\Lambda$  is a positive definite function and  $d\Lambda/dt < 0$  is a negative function, then the system is asymptotically stable at the origin of the equilibrium state. It follows that  $e_R \rightarrow 0$  is exponential as  $t \rightarrow \infty$ .

## Results and discussion

For the numerical simulations, the fourth-order Runge-Kutta method is used to solve the novel system (6). The bifurcation parameter value of the novel chaotic system (6) is taken as in the chaotic case, i. e.  $R = 58$ . The control gains are chosen as  $k_1 = 7$ ,  $k_2 = 4$ ,  $k_3 = 3$ ,  $k_4 = 3$ ,  $k_5 = 4$ ,  $k_6 = 6$ ,  $k_7 = 8$ , and  $k_8 = 11$ . The initial values of the chaotic system (6) are taken as

$$x_1(0) = x_2(0) = x_3(0) = x_4(0) = x_5(0) = x_6(0) = x_7(0) = x_8(0) = 1.$$

The initial value of the parameter estimate is taken as  $R(0) = 59$ .

**Figure 2** shows the time history of the controlled novel chaotic system. It is proved that the controlled system (6) is globally exponentially stable when the adaptive control law (7) and the parameter update law (12) are implemented.

For numerical simulations, the bifurcation parameter value of the novel drive system (3) and the novel response system (13) is taken as in the chaotic case, viz.  $R = 58$ . We take the gain constants as  $k_1 = 3$ ,  $k_2 = 3$ ,  $k_3 = 4$ ,  $k_4 = 2$ ,  $k_5 = 4$ ,  $k_6 = 6$ ,  $k_7 = 8$ , and  $k_8 = 10$ .

The initial conditions of the drive system (3) are taken

$$x_1(0) = x_2(0) = x_3(0) = x_4(0) = x_5(0) = x_6(0) = x_7(0) = x_8(0) = 1$$

The initial values of the response system (13) are chosen as

$$y_1(0) = y_2(0) = y_3(0) = y_4(0) = y_5(0) = y_6(0) = y_7(0) = y_8(0) = 5$$

The initial condition of the bifurcation parameter estimate is taken as  $R(0) = 60$ .

The timing diagrams of  $x_1 - y_1, x_2 - y_2, x_3 - y_3, x_4 - y_4, x_5 - y_5, x_6 - y_6, x_7 - y_7, x_8 - y_8$  are shown in **Figures 3** and **4**. **Figures 3** and **4** describe the complete synchronization of the identical novel chaotic systems (3) and (13). **Figure 5** shows the convergence of the synchronization errors  $\zeta_1, \zeta_2, \zeta_3, \zeta_4, \zeta_5, \zeta_6, \zeta_7, \zeta_8$  to zero exponentially with time.

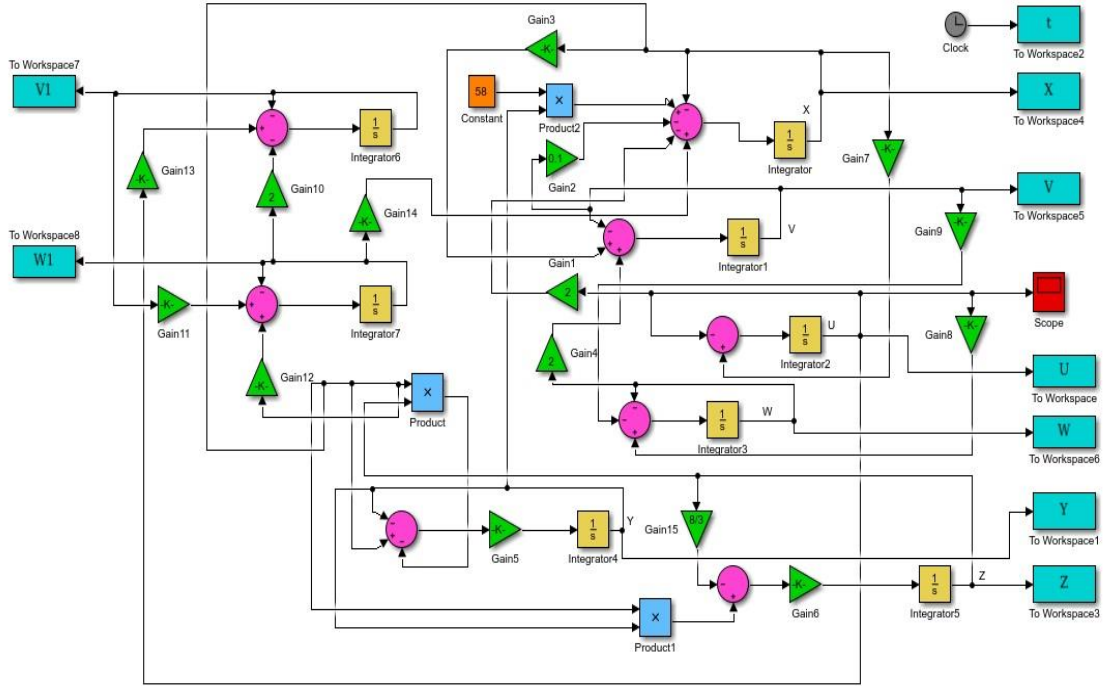


**Figure 6** Matlab-Simulink model for equations (3). The simulation data is displayed using the To Workspace blocks.

#### Matlab-Simulink model

The equations (3) were numerically solved using the model developed by Matlab-Simulink. The Matlab-Simulink model of a chaotic oscillation generator consists of interconnected blocks of amplification, summation, subtraction, multiplication, integration, and signal recording devices. **Figure 6** shows a diagram of the Matlab-Simulink model. **Figures 7** and **8** show the results of modeling the system of equations (3) for the parameter  $R = 58$ . On the phase portraits of **Figures 7** and **8** one can see the complexity of trajectories, which is characteristic of strange attractors.

Note that a direct implementation of (3) with an electronic circuit presents one certain difficulty. The dynamic variables  $x_1, x_5, x_6, x_7, x_8$  in (3) occupy a wide dynamic range with values that exceed reasonable power supply limits. The operating voltage range of operational amplifiers is typically  $-15V$  to  $+15V$  in practical electronic circuits. This problem was proposed to be eliminated by a simple transformation of variables of the dynamic system [4]. For our case, we need to rescale the following variables:  $x_1 = 10X_1, x_5 = 20X_5, x_6 = 10X_6, x_7 = 10X_7, x_8 = 5X_8$ . The rest of variables are simply redesignated  $x_2 = X_2, x_3 = X_3, x_4 = X_4$ . With this scaling, equations (3) for are transformed

$$\begin{cases} \dot{X}_1 = -X_1 + 5.8X_2 - 0.2X_4 - 0.2X_5 + 0.03X_8 \\ \dot{X}_2 = -0.1X_2 + X_1 - X_1X_3 \\ \dot{X}_3 = -\frac{8}{30}X_3 + X_1X_2 \\ \dot{X}_4 = -X_4 + X_1 \\ \dot{X}_5 = -X_5 + 4.12X_1 + X_6 \\ \dot{X}_6 = -X_6 - 2.465X_4 - 0.2X_5 \\ \dot{X}_7 = -X_7 + 2.84X_4 - X_8 \\ \dot{X}_8 = -X_8 + 0.94X_1 + 0.2X_7 \end{cases} \quad (20)$$

Note that two systems (3) and (20) are equivalent since the linear transformation does not change the physical properties of nonlinear systems. The chaotic solutions of the equations (20) obtained using the

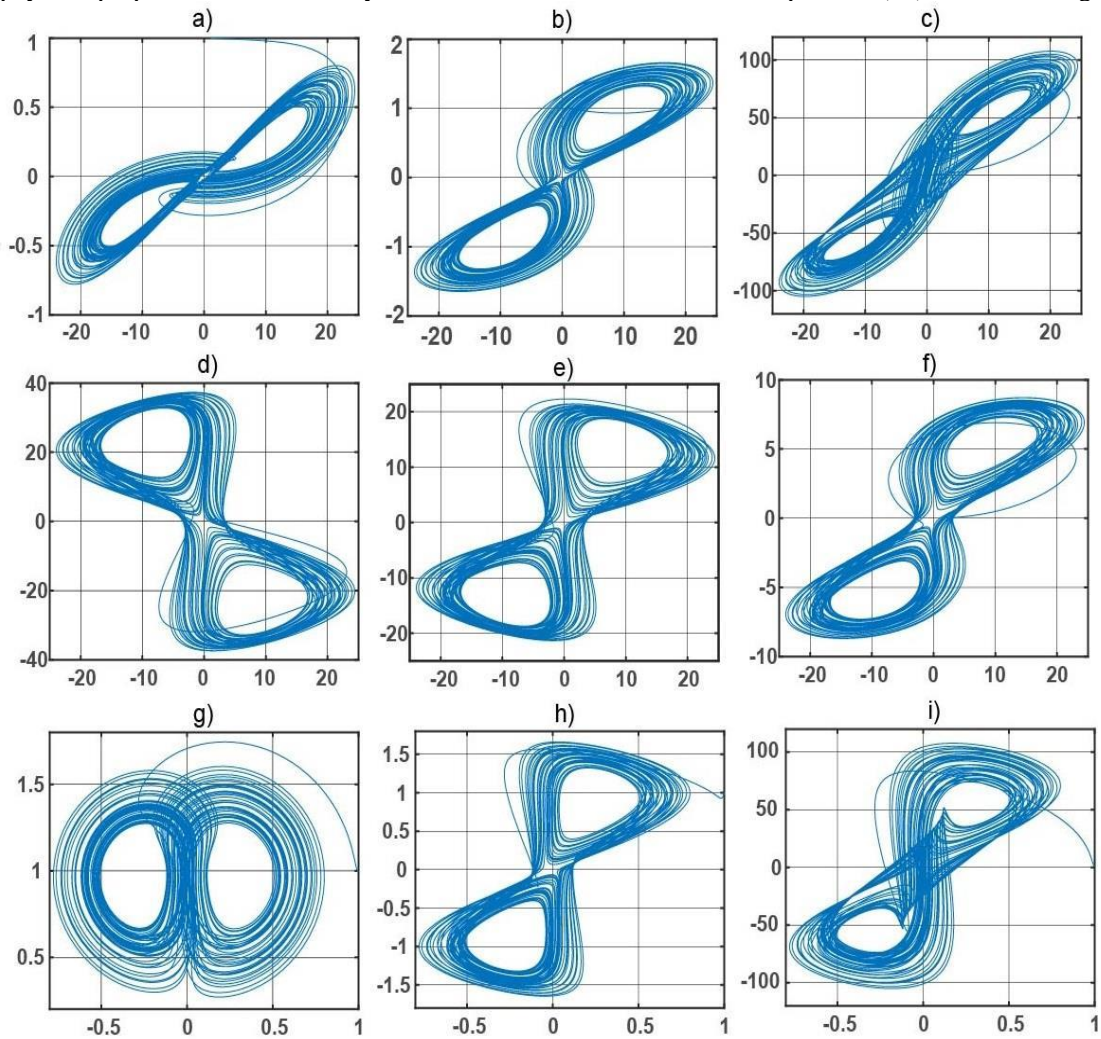


**Figure 7** The phase portraits in the planes a)  $x_1x_2$ , b)  $x_1x_4$ , c)  $x_1x_5$ , d)  $x_1x_6$ , e)  $x_1x_7$ , f)  $x_1x_8$ , g)  $x_2x_3$ , h)  $x_2x_4$ , i)  $x_2x_5$ .

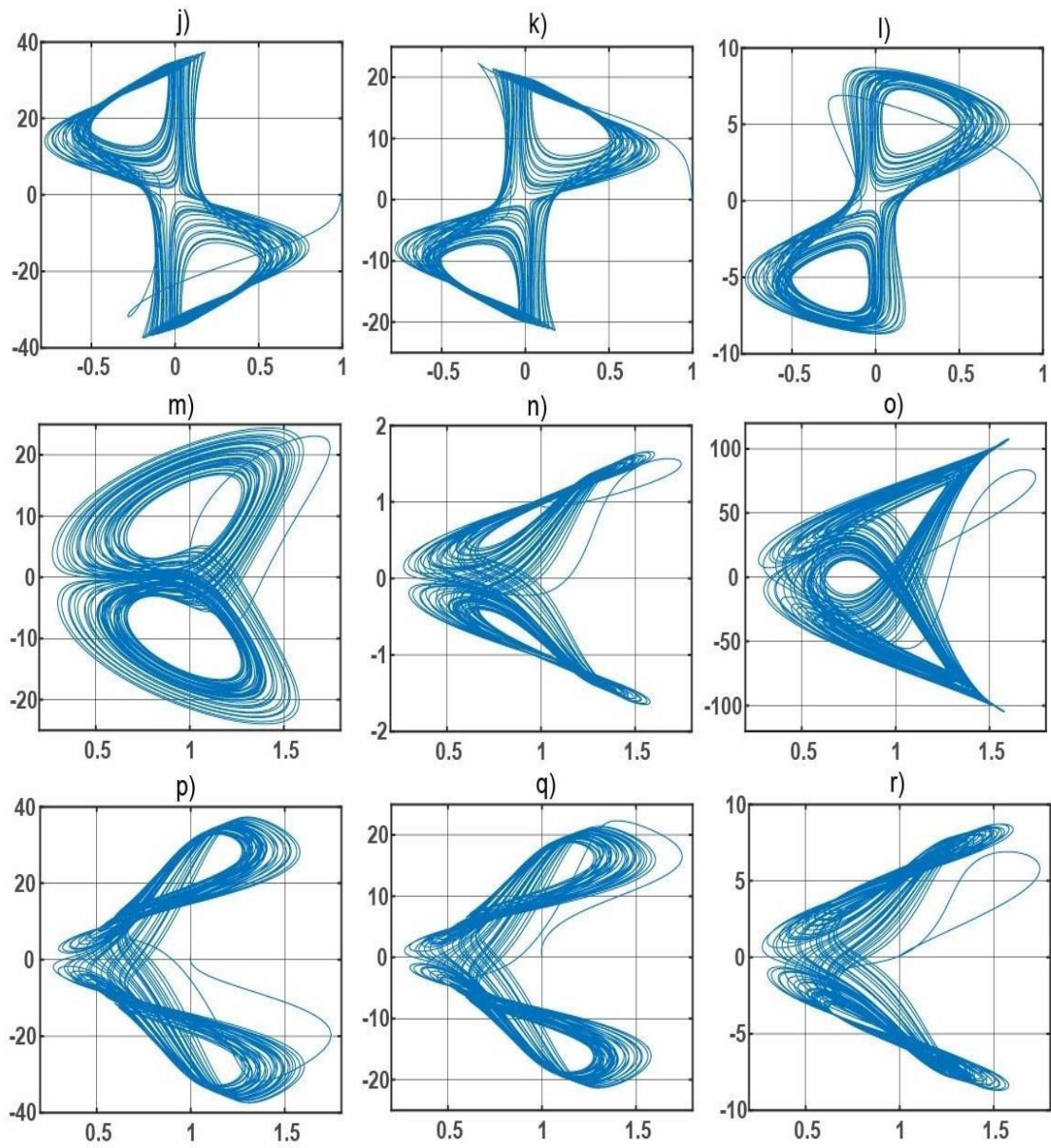


**Figure 8** The phase portraits in the planes j)  $x_2x_6$ , k)  $x_2x_7$ , l)  $x_2x_8$ , m)  $x_3x_1$ , n)  $x_3x_4$ , o)  $x_3x_5$ , p)  $x_3x_6$ , q)  $x_3x_7$ , r)  $x_3x_8$ .

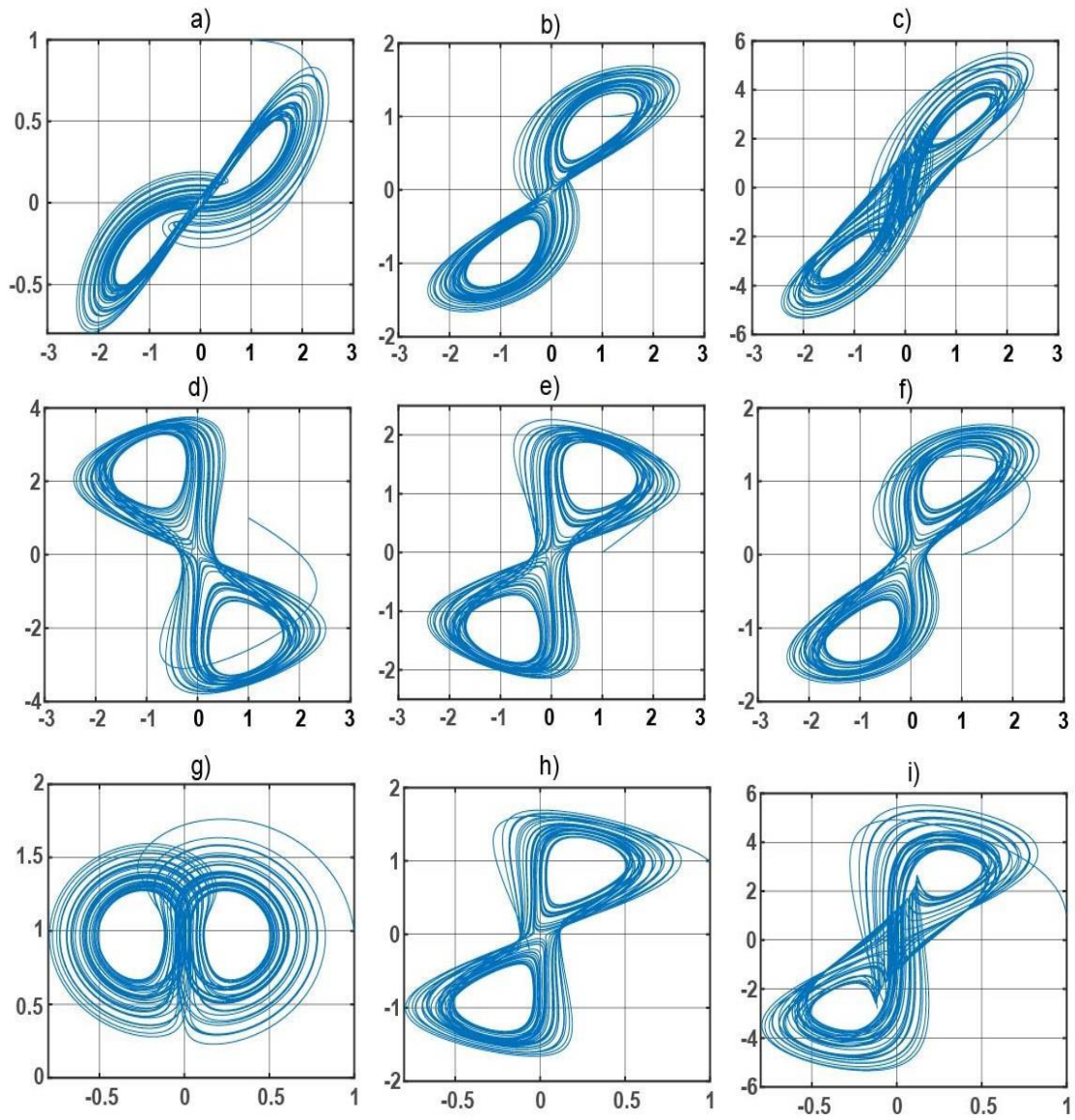


**Figure 9** The phase portraits in the planes a)  $X_1X_2$ , b)  $X_1X_4$ , c)  $X_1X_5$ , d)  $X_1X_6$ , e)  $X_1X_7$ , f)  $X_1X_8$ , g)  $X_2X_3$ , h)  $X_2X_4$ , i)  $X_2X_5$ .

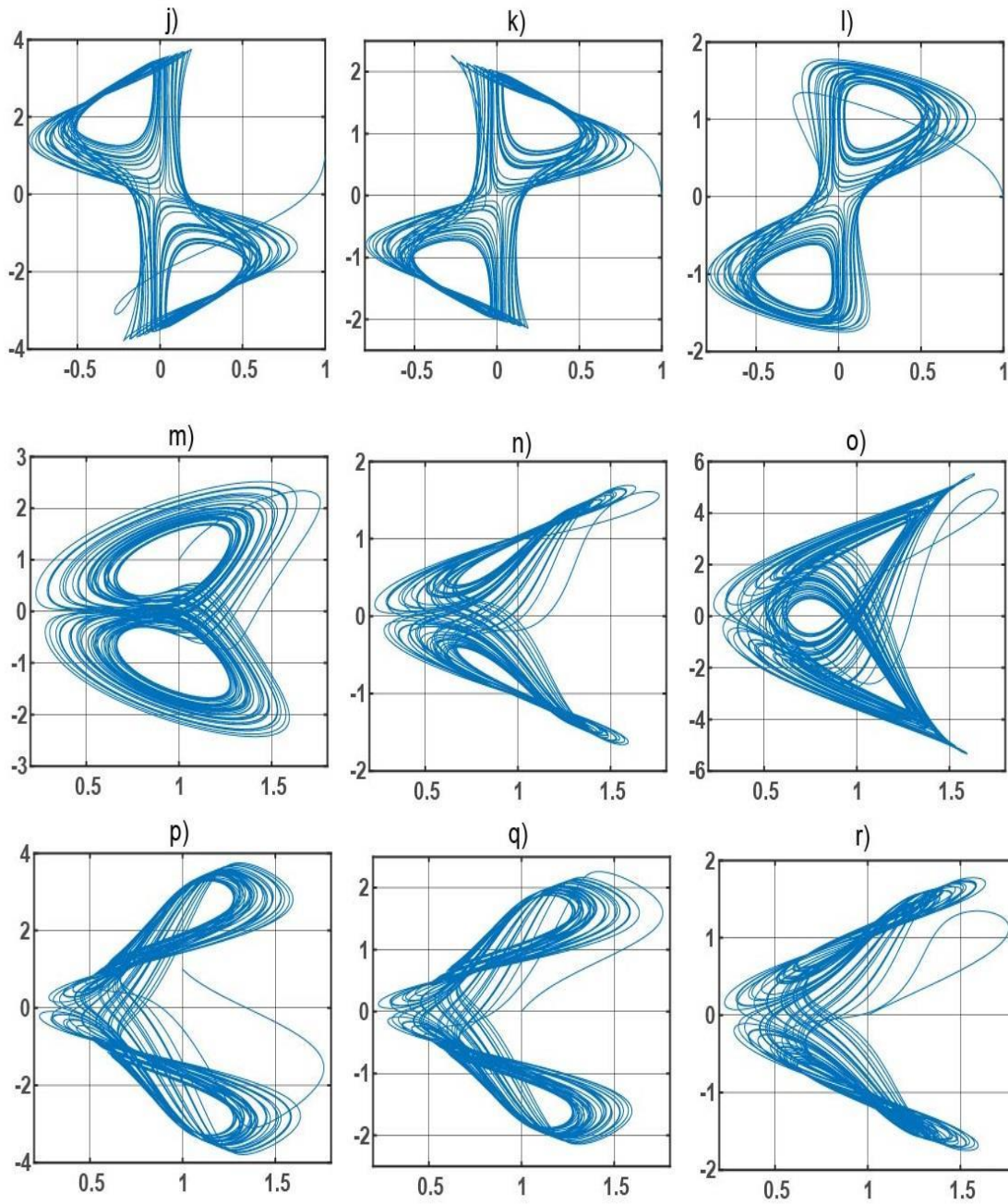


**Figure 10** The phase portraits in the planes j)  $X_2X_6$ , k)  $X_2X_7$ , l)  $X_2X_8$ , m)  $X_3X_1$ , n)  $X_3X_4$ , o)  $X_3X_5$ , p)  $X_3X_6$ , q)  $X_3X_7$ , r)  $X_3X_8$ .

Matlab-Simulink model are shown in **Figures 9** and **10**. It can be seen that the range of values of dynamic variables has significantly decreased compared to the values of dynamic variables on the graphs of chaotic solutions of equations (20) in **Figures 9** and **10**.

#### *LabView model*

Of great interest is the modeling of nonlinear dynamic systems using various software environments,

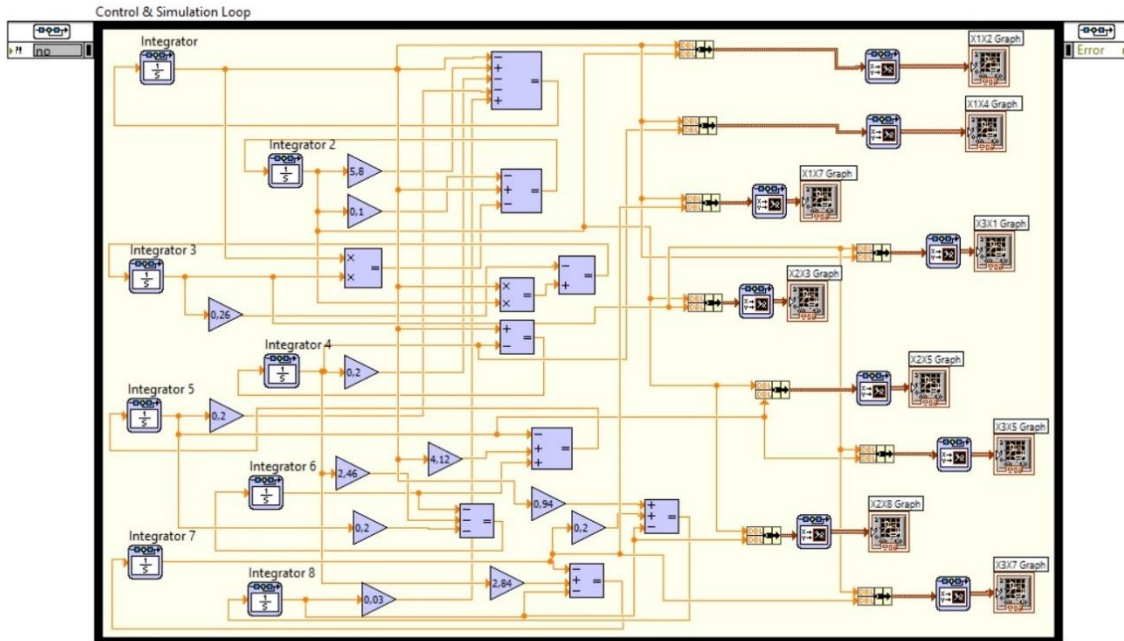


**Figure 11** Block diagram implementing chaotic system (6) in LabView.

which makes it possible to demonstrate various informational properties of chaotic oscillations. To simulate a chaotic system (20) and demonstrate the results, we use the LabView software environment. LabView is a graphical software platform that is now very widely used in engineering applications [28]. For the development of algorithms in LabView, a visual platform has been created. **Figure 11** shows a block diagram of the chaotic system (20). This model is created using Control & Simulation toolbox in LabView. As can be seen from **Figure 11**, for modeling differential equations (20) operations of addition, multiplication, multiplication on a fixed number, integration were used. **Figure 12** shows a programming interface that displays these properties of information modeling in the form of phase portraits in the planes  $X_1X_2, X_1X_4, X_1X_7, X_2X_3, X_2X_5, X_2X_8, X_3X_1, X_3X_5, X_3X_7$  for the initial conditions  $X_1(0) = X_2(0) = X_3(0) = X_4(0) = X_5(0) = X_6(0) = X_7(0) = X_8(0) = 1$ . Comparing phase portraits in **Figures 9** and **10** and **Figure 12** can be seen that the results of modeling in Matlab-Simulink and LabView the chaotic system (20) coincide.

#### Circuit Simulation

The circuit implementation of chaotic systems is an important task in engineering applications such as secure communications and random bits generation. The simple circuit implementation of the dynamic system of equations (20) will be composed of six operational amplifiers performing the signal integration function. Dynamic system variables (20) are represented by appropriate electrical signals that correspond to instantaneous voltage values  $U_1(\tau), U_2(\tau), U_3(\tau), U_4(\tau), U_5(\tau), U_6(\tau), U_7(\tau), U_8(\tau)$  on capacitors  $C_1, C_2, C_3, C_4, C_5, C_6, C_7, C_8$ . The electrical analog of the system (20) in accordance with the laws of Kirchhoff for electrical circuits takes the following form

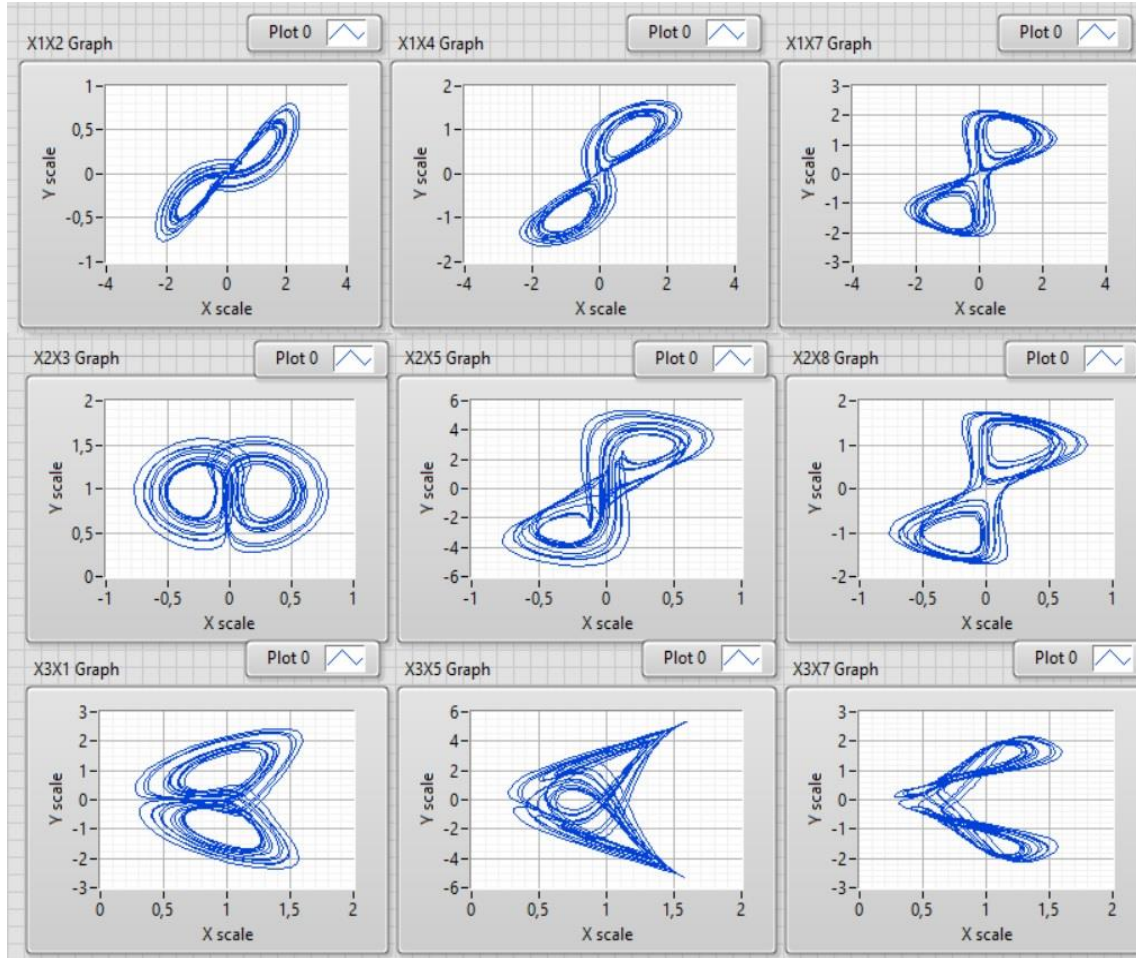


**Figure 12** Phase portraits are simulated in LabView.

$$\left\{ \begin{array}{l}
 C_1 \frac{dU_1}{d\tau} = -\frac{U_1}{R_{11}} + \frac{U_2}{R_{12}} - \frac{U_4}{R_{13}} - \frac{U_5}{R_{14}} + \frac{U_8}{R_{15}} \\
 C_2 \frac{dU_2}{d\tau} = -\frac{U_2}{R_{21}} + \frac{U_1}{R_{22}} - \frac{U_1 U_3}{R_{23} K} \\
 C_3 \frac{dU_3}{d\tau} = -\frac{U_3}{R_{31}} + \frac{U_1 U_2}{R_{32} K} \\
 C_4 \frac{dU_4}{d\tau} = -\frac{U_4}{R_{41}} + \frac{U_1}{R_{42}} \\
 C_5 \frac{dU_5}{d\tau} = -\frac{U_5}{R_{51}} + \frac{U_1}{R_{52}} + \frac{U_6}{R_{53}} \\
 C_6 \frac{dU_6}{d\tau} = -\frac{U_6}{R_{61}} - \frac{U_4}{R_{62}} - \frac{U_5}{R_{63}} \\
 C_7 \frac{dU_7}{d\tau} = -\frac{U_7}{R_{71}} + \frac{U_4}{R_{72}} - \frac{U_8}{R_{73}} \\
 C_8 \frac{dU_8}{d\tau} = -\frac{U_8}{R_{81}} + \frac{U_1}{R_{82}} + \frac{U_7}{R_{83}}
 \end{array} \right. \quad (21)$$

where  $R_{ij}$  are resistors ( $i, j = 1, 2, 3, 4, 5, 6, 7, 8$ );  $K$  is a scale coefficient for the multiplier. We choose the normalized resistor as  $R_0 = 10 \text{ k}\Omega$ , and the normalized capacitor as  $C_0 = 100 \text{ nF}$ . Then the time constant is equal to  $t_0 = R_0 C_0 = 10^{-3} \text{ s}$ . We rescale the state variables of the system (21) as follows

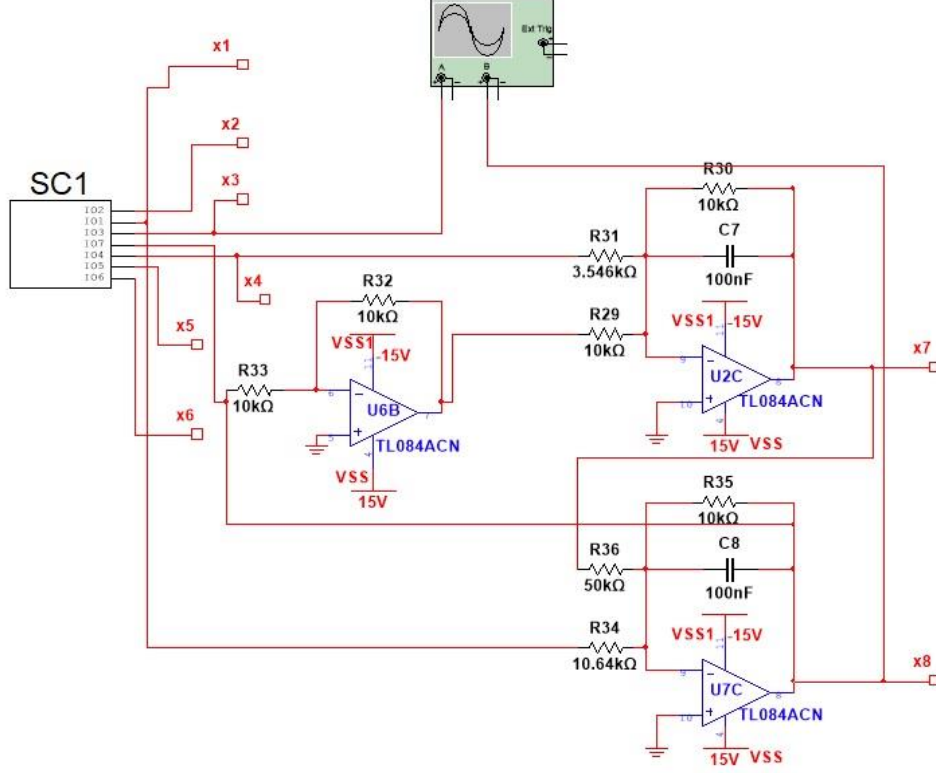


**Figure 13** Electronic circuit of the generator of chaotic oscillations based on the system of equations (23).

$U_1 = U_0 \tilde{X}_1, U_2 = U_0 \tilde{X}_2, U_3 = U_0 \tilde{X}_3, U_4 = U_0 \tilde{X}_4, U_5 = U_0 \tilde{X}_5, U_6 = U_0 \tilde{X}_6, U_7 = U_0 \tilde{X}_7, U_8 = U_0 \tilde{X}_8$  and  $K = U_0 K'$ ,  $\tau = t_0 t$  write equations (21) in a dimensionless form

$$\begin{cases}
 \frac{C_1}{C_0} \frac{d\tilde{X}_1}{dt} = -\frac{R_0}{R_{11}} \tilde{X}_1 + \frac{R_0}{R_{12}} \tilde{X}_2 - \frac{R_0}{R_{13}} \tilde{X}_4 - \frac{R_0}{R_{14}} \tilde{X}_5 + \frac{R_0}{R_{15}} \tilde{X}_8 \\
 \frac{C_2}{C_0} \frac{d\tilde{X}_2}{dt} = -\frac{R_0}{R_{21}} \tilde{X}_2 + \frac{R_0}{R_{22}} \tilde{X}_1 - \frac{R_0}{R_{23} K'} \tilde{X}_1 \tilde{X}_3 \\
 \frac{C_3}{C_0} \frac{d\tilde{X}_3}{dt} = -\frac{R_0}{R_{31}} \tilde{X}_3 + \frac{R_0}{R_{32} K'} \tilde{X}_1 \tilde{X}_2 \\
 \frac{C_4}{C_0} \frac{d\tilde{X}_4}{dt} = -\frac{R_0}{R_{41}} \tilde{X}_4 + \frac{R_0}{R_{42}} \tilde{X}_1 \\
 \frac{C_5}{C_0} \frac{d\tilde{X}_5}{dt} = -\frac{R_0}{R_{51}} \tilde{X}_5 + \frac{R_0}{R_{52}} \tilde{X}_1 + \frac{R_0}{R_{53}} \tilde{X}_6 \\
 \frac{C_6}{C_0} \frac{d\tilde{X}_6}{dt} = -\frac{R_0}{R_{61}} \tilde{X}_6 - \frac{R_0}{R_{62}} \tilde{X}_4 - \frac{R_0}{R_{63}} \tilde{X}_5 \\
 \frac{C_7}{C_0} \frac{d\tilde{X}_7}{dt} = -\frac{R_0}{R_{71}} \tilde{X}_7 + \frac{R_0}{R_{72}} \tilde{X}_4 - \frac{R_0}{R_{73}} \tilde{X}_8 \\
 \frac{C_8}{C_0} \frac{d\tilde{X}_8}{dt} = -\frac{R_0}{R_{81}} \tilde{X}_8 + \frac{R_0}{R_{82}} \tilde{X}_1 + \frac{R_0}{R_{83}} \tilde{X}_7
 \end{cases} \quad (22)$$

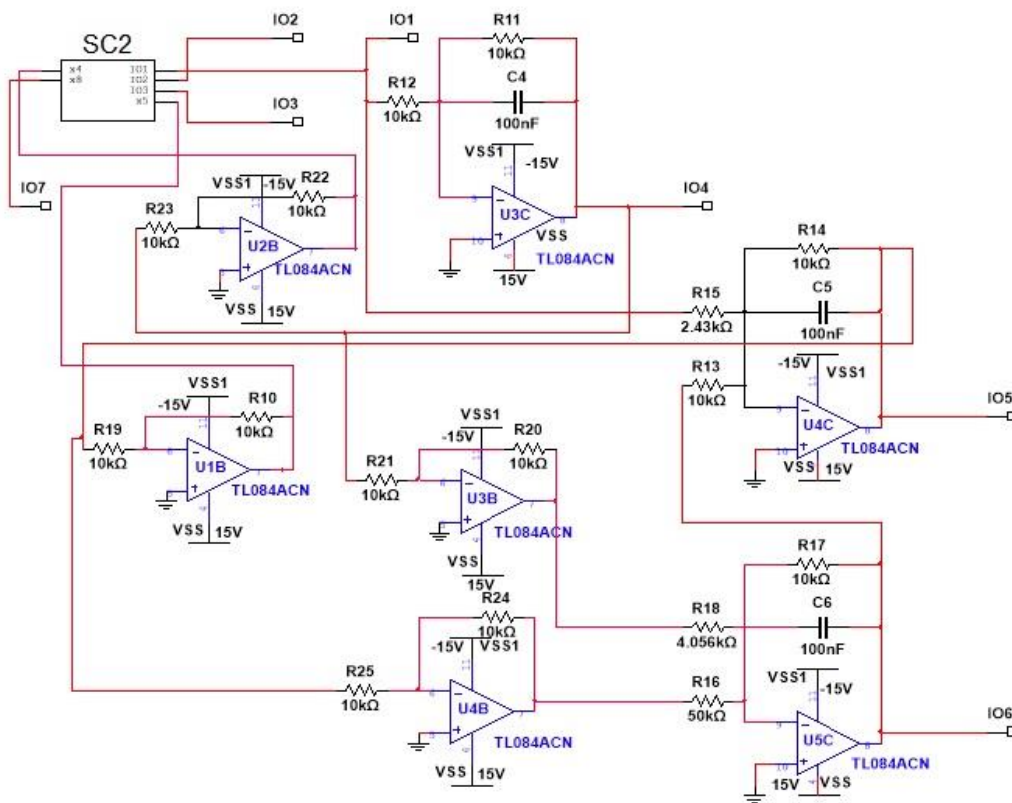


Figure 14 Electronic circuit of the subsystem SC1.

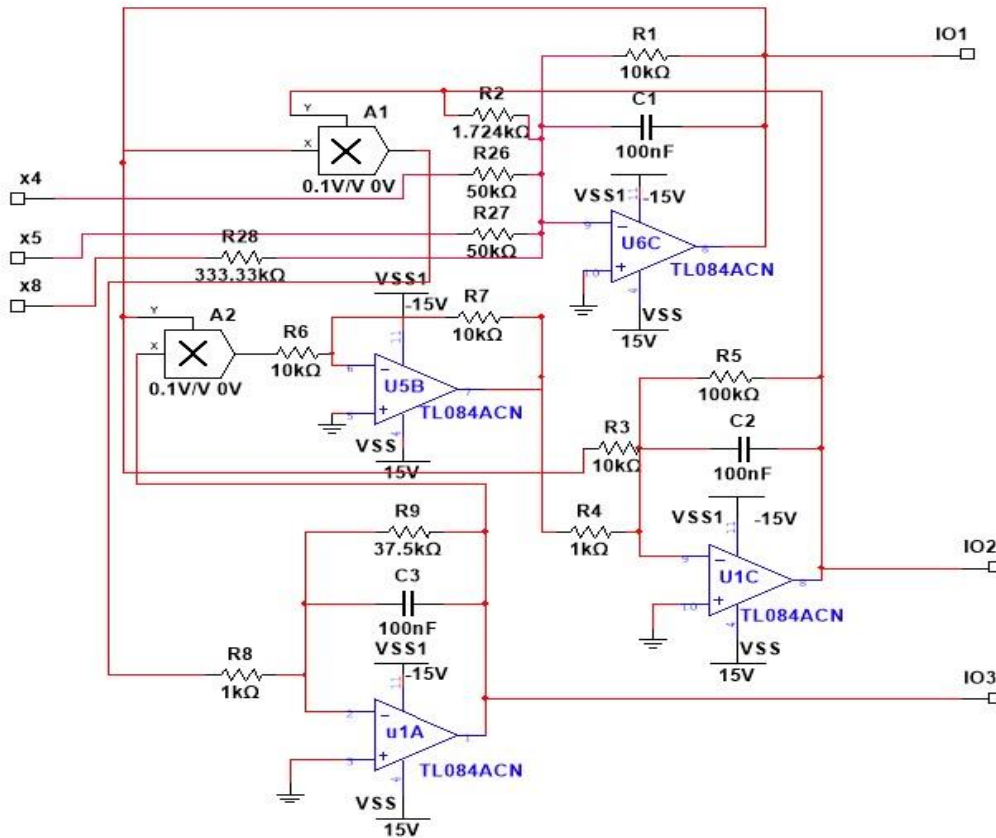
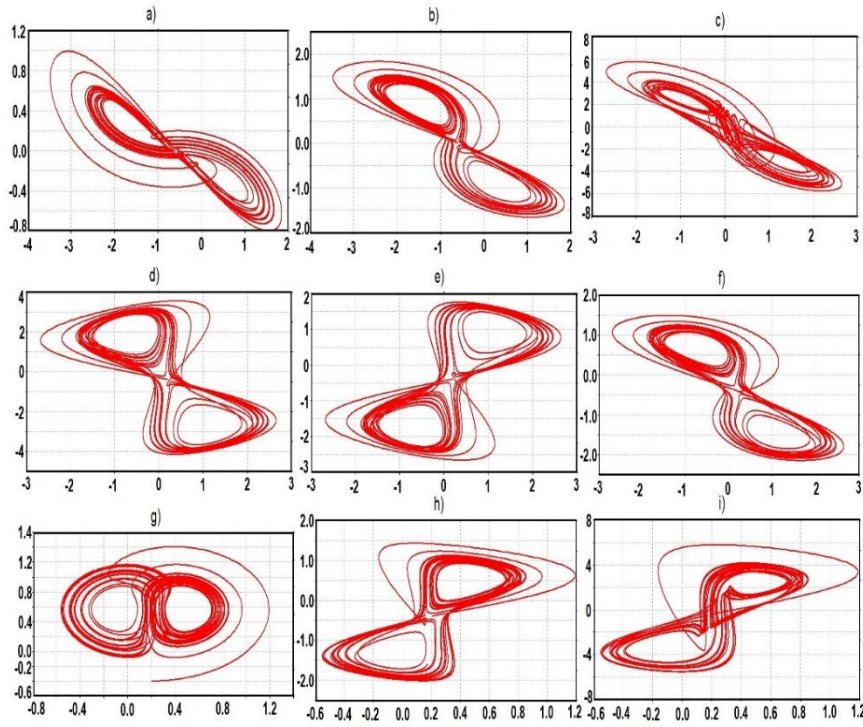
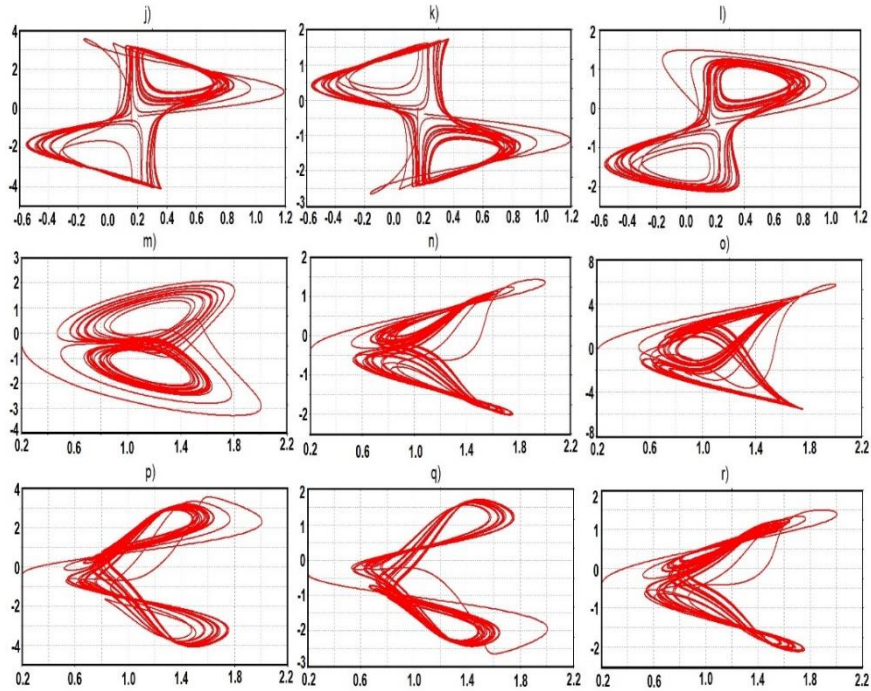


Figure 15 Electronic circuit of the subsystem SC2.

Substituting  $R_0 = 10 \text{ k}\Omega$ ,  $C_1 = C_2 = C_3 = C_4 = C_5 = C_6 = C_7 = C_8 = C_0 = 100 \text{ nF}$  and  $K' = 10$  into (22) and comparing numerical values before the output voltages of the system (22) and (20), we get the value of electronic circuit resistors



**Figure16** Chaotic phase trajectories displayed in Multisim oscilloscopes: a)  $\tilde{X}_1\tilde{X}_2$ , b)  $\tilde{X}_1\tilde{X}_4$ , c)  $\tilde{X}_1\tilde{X}_5$ , d)  $\tilde{X}_1\tilde{X}_6$ , e)  $\tilde{X}_1\tilde{X}_7$ , f)  $\tilde{X}_1\tilde{X}_8$ , g)  $\tilde{X}_2\tilde{X}_3$ , h)  $\tilde{X}_2\tilde{X}_4$ , i)  $\tilde{X}_2\tilde{X}_5$ .



**Figure17** Chaotic phase trajectories displayed in Multisim oscilloscopes: j)  $\tilde{X}_2\tilde{X}_6$ , k)  $\tilde{X}_2\tilde{X}_7$ , l)  $\tilde{X}_2\tilde{X}_8$ ,

m)  $\tilde{X}_3\tilde{X}_1$ , n)  $\tilde{X}_3\tilde{X}_4$ , o)  $\tilde{X}_3\tilde{X}_5$ , p)  $\tilde{X}_3\tilde{X}_6$ , q)  $\tilde{X}_3\tilde{X}_7$ , r)  $\tilde{X}_3\tilde{X}_8$ .

$$\left\{ \begin{aligned} \frac{d\tilde{X}_1}{dt} &= -\frac{10k}{10k}\tilde{X}_1 + \frac{10k}{1.724k}\tilde{X}_2 - \frac{10k}{50k}\tilde{X}_4 - \frac{10k}{50k}\tilde{X}_5 + \frac{10k}{333.33k}\tilde{X}_8 \\ \frac{d\tilde{X}_2}{dt} &= -\frac{10k}{100k}\tilde{X}_2 + \frac{10k}{10k}\tilde{X}_1 - \frac{10k}{1k \cdot 10}\tilde{X}_1\tilde{X}_3 \\ \frac{d\tilde{X}_3}{dt} &= -\frac{10k}{37.5k}\tilde{X}_3 + \frac{10k}{1k \cdot 10}\tilde{X}_1\tilde{X}_2 \\ \frac{d\tilde{X}_4}{dt} &= -\frac{10k}{10k}\tilde{X}_4 + \frac{10k}{10k}\tilde{X}_1 \\ \frac{d\tilde{X}_5}{dt} &= -\frac{10k}{10k}\tilde{X}_5 + \frac{10k}{2.43k}\tilde{X}_1 + \frac{10k}{10k}\tilde{X}_6 \\ \frac{d\tilde{X}_6}{dt} &= -\frac{10k}{10k}\tilde{X}_6 - \frac{10k}{4.056k}\tilde{X}_4 - \frac{10k}{50k}\tilde{X}_5 \\ \frac{d\tilde{X}_7}{dt} &= -\frac{10k}{10k}\tilde{X}_7 + \frac{10k}{3.546k}\tilde{X}_4 - \frac{10k}{10k}\tilde{X}_8 \\ \frac{d\tilde{X}_8}{dt} &= -\frac{10k}{10k}\tilde{X}_8 + \frac{10k}{10.64k}\tilde{X}_1 + \frac{10k}{50k}\tilde{X}_7 \end{aligned} \right. \quad (23)$$

We use the computer environment Multisim for a circuit implementation of the generator of chaotic oscillations of the system (23), where the role of integrators is played by operational amplifiers. We will design an electronic circuit using standard methods of turning on operational amplifiers according to integrating, summing, and inverting signals. The analog circuit of the system (23) was presented in **Figure 13**. For convenience, we use the subsystem SC1 for the first six equations (23). The electronic circuit of the subsystem SC1 is shown in **Figure 14**. The subsystem SC1 includes another subsystem SC2, which for the first three equations of system (23) (like Lorentz equations) is constructed. The electronic circuit of the subsystem SC2 is shown in **Figure 15**. It can be seen that the circuits are obtained based on operational amplifiers TL084ACN and analog multipliers A1 and A2 (for example AD633 series). Terminals x1,x2,x3,x4,x5,x6,x7,x8 on the diagram (see **Figure 13**) correspond to signal outputs  $\tilde{X}_1, \tilde{X}_2, \tilde{X}_3, \tilde{X}_4, \tilde{X}_5, \tilde{X}_6, \tilde{X}_7, \tilde{X}_8$ . By connecting a dual-channel oscilloscope to different outputs, we get different phase portraits in the Multisim environment, which are shown in **Figure 16**. As it can be seen from the MultiSim outputs in **Figure 16** and Matlab-Simulink in **Figures 9** and **10** and LabView in **Figure 12**, the results are similar.

## Conclusions

In this work, we complemented the dynamic analysis of the new 8-dimensional chaotic system from the article [21], i.e. the fundamental properties of the system such as Lyapunov exponents and Kaplan-Yorke dimension, as well as its phase portraits, were described in detail. An adaptive controller for stabilizing the proposed system with unknown parameters and the chaos synchronization of two identical chaotic systems was studied. We designed Matlab-Simulink and LabView models for numerical simulation of equations of nonlinear dynamics of nonuniformly rotating convection of an electrically conductive fluid in a helical magnetic field. According to the phase portraits obtained as a result of Matlab-Simulink and LabView simulation, it was found that the oscillations arising in the systems have a complex chaotic character. For a novel 8D chaotic system, an electronic circuit of a chaos generator was designed. The performance of this electronic circuit was tested in the Multisim environment.

Experimental implementation of new chaos generators will be useful in designing multichannel devices for the secure transmission of information.

## References

- [1] MP Kennedy, R Rovatti and G Setti. *Chaotic Electronics in Telecommunications*. CRC Press, London, 2000, 442 p.

- [2] O Boubaker and S Jafari. *Recent advances in Chaotic systems and synchronization: from theory to real world applications*. Academic Press, London, 2019, 392 p.
- [3] EN Lorenz. Deterministic non-periodic flow. *J. Atmos. Sci.* 1963; **20**, 130-142.
- [4] KM. Cuomo and AV Oppenheim. Circuit implementation of synchronized chaos with applications to communications. *Phys. Rev. Letters* 1993; **71**, 65-68.
- [5] A Sambas, WSM Sanjaya and M Mamat. Design and analysis bidirectional chaotic synchronization of Rossler circuit and its application for secure communication. *Appl. Math. Sci.* 2013; 11-21.
- [6] KM Ibrahim, RK Jamal and F H Ali. Chaotic behavior of the Rossler model and its analysis by using bifurcations of limit cycles and chaotic attractors. IOP Conf. Series: Journal of Physics: Conf. Series 1003, 012099, 2018.
- [7] I Pehlivan, Y Uyaroglu. Rikitake Attractor and its Synchronization Application for Secure Communication Systems. *J. Appl. Sci.* 2007; **7**, 232-236.
- [8] I Pehlivan, Y Uyaroglu. Simplified Chaotic Diffusionless Lorenz Attractor and its Application to Secure Communication Systems. *IET Commun.* 2007; **1**, 1015-1022.
- [9] I Pehlivan, Y Uyaroglu. A New Chaotic Attractor from General Lorenz System Family and its Electronic Experimental Implementation. *Turk J. Elec. Eng. & Comp. Sci.* 2010; **18**, 171-184.
- [10] QH. Alsafasfeh, MS Al-Arni. A New Chaotic Behavior from Lorenz and Rossler Systems and Its Electronic Circuit Implementation. *SCIRP Circuits and Systems* 2011; **2**, 101-105.
- [11] S Vaidyanathan, K Rajagopal, ChK. Volos, IM. Kyprianidis, and IN. Stouboulos. Analysis, Adaptive Control and Synchronization of a Seven-Term Novel 3D Chaotic System with Three Quadratic Nonlinearities and its Digital Implementation in LabVIEW. *J. Eng. Sci. Technol. Rev.* 2015; **8**, 130-141.
- [12] A Sambas, S Vaidyanathan, M Mamat, M Sanjaya WS, SH Yuningsih, K Zakaria and Subiyanto. Dynamics, Circuit Design and Fractional-Order Form of a Modified Rucklidge Chaotic System. *J. Phys.: Conf. Ser.* 2018; **1090**, 012038.
- [13] W Fa-Qiang, L Chong-Xin. Hyperchaos evolved from the Liu chaotic system. *Chinese Phys.* 2006; **15**, 963-968.
- [14] L Xiao-Hua, L Xiao-Hua at al. Circuitry implementation of a novel four-dimensional nonautonomous hyperchaotic Liu system and its experimental studies on synchronization control. *Chin. Phys. B* 2009; **18**, 2168-2175.
- [15] J Lu, G Chen, S Zhang. The compound structure of a new chaotic attractor. *Chaos Solitons Fractals* 2002; **14**, 669-672.
- [16] L Xiong, Z Liu, and X Zhang. Dynamical Analysis, Synchronization, Circuit Design, and Secure Communication of a Novel Hyperchaotic System. *Hindawi Complexity* 2017; Article ID 4962739, 23 pages. <https://doi.org/10.1155/2017/4962739>
- [17] L Xiong, Yan-Jun Lu, Qi-Meng Zhang, and Zhi-Yu Zhang. Circuit Implementation and Antisynchronization of an Improved Lorenz Chaotic System. *Hindawi Shock and Vibration* 2016; Article ID 1617570, 12 pages. <https://doi.org/10.1155/2016/1617570>
- [18] S. Vaidyanathan, ChK Volos, and VT. Pham. Analysis, Control, Synchronization and SPICE Implementation of a Novel 4D Hyperchaotic Rikitake Dynamo System without Equilibrium. *J. Eng. Sci. Technol. Rev.* 2015; **8**, 232-244.
- [19] S Vaidyanathan, VT Pham, and CK Volos. A 5D hyperchaotic Rikitake dynamo system with hidden attractors. *Eur. Phys. J. Special. Topics* 2015; **224**, 1575-1592.
- [20] S Vaidyanathan et al. A 5D Multi-Stable Hyperchaotic Two-Disk Dynamo System with no Equilibrium Point: Circuit Design, FPGA Realization and Applications to TRNGs and Image Encryption. *IEEE Access* 2021; **9**, 81352-81369.

- [21] E Tlelo-Cuautle, L Gerardo de la Fraga, O Guillén-Fernández, and A Silva-Juárez. Optimization of Integer /Fractional Order Chaotic Systems by Metaheuristics and their Electronic Realization, Taylor & Francis Group, LLC, 2021.
- [22] MI Kopp, AV Tur, VV Yanovsky. Magnetic convection in a nonuniformly rotating electrically conductive medium in an external spiral magnetic field. *Fluid Dyn. Res.* 2021; **53**, 015509.
- [23] MI Kopp, AV Tur, and VV Yanovsky. Magnetic Convection in a Nonuniformly Rotating Electroconducting Medium. *J. Exp. Theor. Phys.* 2018; **127**, 1173-1196.
- [24] G Benettin, L Galgani, A Giorgilli, and JM Strelcyn. Lyapunov characteristic exponents for smooth dynamical systems and for Hamiltonian systems: A method for computing all of them. *Meccanica* 1980; **15**, 9-30.
- [25] A Wolf, JB Swift, HL Swinney, and JA Vastano. Determining Lyapunov Exponents from a Time Series. *Phys. D: Nonlinear Phenom.* 1985; **16**, 285-317.
- [26] M Sandri. Numerical Calculation of Lyapunov Exponents. *Mathematica J.* 1996; **6**, 78-84. <http://www.mathematica-journal.com/issue/v6i3/article/sandri/contents/63sandri.pdf>
- [27] H Binous and N Zakia. An Improved Method for Lyapunov Exponents Computation. March 9, 2008. <https://library.wolfram.com/infocenter/MathSource/7109/>
- [28] RW Larsen. *LabVIEW for Engineers*. Montana State University. Prentice Hall. Boston Columbus Indianapolis New York San Francisco Upper Saddle River, 2011, 406 p.